doi.org/10.36721/PJPS.2024.37.6.REG.1443-1454.1

Lycorine attenuates lipopolysaccharide-induced inflammation and intestinal epithelial barrier dysfunction in Caco-2 cells through inhibiting the STING/NF-κB pathway

Weiwei Gao[1], Peng Guan[1], Wanpeng Gao[1] and Xiaodan Li[2]*

[1]Emergency Department of the Second Affiliated Hospital of Tianjin University of Traditional Chinese Medicine, No.69, Increment Road, Hebei District, Tianjin, China

[2]Respiratory Department, the Second Affiliated Hospital of Tianjin University of Traditional Chinese Medicine, No.69, Increment Road, Hebei District, Tianjin, China

Abstract: Lycorine (LYC) is an isoquinoline alkaloid known for its various biological effects like anti-viral and anti-inflammatory. The purpose of this research was to offer a reference for the clinical application of LYC in inflammatory bowel disease. The toxicity of LYC on Caco-2 cells was assessed utilizing CCK-8 assay and Lactate dehydrogenase (LDH) kit. Tunel staining and flow cytometry determined apoptosis, and Elisa kits measured levels of inflammatory factors. Trans-endothelial electrical resistance (TEER) assay and FITC-dextran assay for Caco-2 cell permeability. Western blot assessed the levels of inflammation-related and stimulator of interferon genes (STING)/nuclear factor kappaB (NF-κB) pathway proteins. Caco-2 cell viability and LDH release were not impacted by LYC concentrations below 20μM and LYC (5, 10 and 20μM) attenuated inflammation and apoptosis in Caco-2 cells induced by lipopolysaccharide (LPS). LPS decreased TEER values and increased FITC-dextran levels and LYC ameliorated epithelial barrier dysfunction caused by LPS. LPS activated the STING/NF-κB pathway, which was hindered by LYC. The protective impact of LYC on Caco-2 cells was reduced by over expression STING. In conclusion, LYC reduced cell death and inflammation in Caco-2 cells and preserved the integrity of the epithelial barrier by hindering the STING/NF-κB pathway.

Keywords: Lycorine, intestinal inflammation, epithelial barrier, lipopolysaccharide, stimulator of interferon genes (STING)/nuclear factor kappaB (NF-κB) pathway.

Submitted on 21-08-2024 – Revised on 19-09-2024 – Accepted on 23-10-2024

INTRODUCTION

The intestines serve as both the largest organ for digestion and the primary site for exchanging substances with the external environment (Zhou *et al.*, 2020). Intestinal epithelial cells serve as a barrier, preventing harmful substances and pathogens from entering the body (Chen *et al.*, 2021). The tight junction (TJ) is vital for upholding the integrity of the intestinal barrier and the transmembrane family of proteins (Claudins and Occludins) and the periplasmic family of proteins (Zonula Occuludens) are important components of the TJ (Nighot *et al.*, 2021, Horowitz *et al.*, 2023). An impaired intestinal barrier may cause toxins to escape from the intestines into the blood, resulting in disorders like inflammatory bowel disease (IBD), diabetes mellitus and systemic inflammatory reactions (Saez *et al.*, 2021, Shen *et al.*, 2022). IBD has been reported to affect about 3 million people worldwide and the incidence continues to rise (Mak *et al.*, 2020). The pathogenesis of IBD is convoluted and still not incompletely known. Several researches have demonstrated that IBD is closely associated with impaired TJ (d'Aldebert *et al.*, 2020, Rohr *et al.*, 2020). Therefore, maintaining intestinal epithelial cell barrier integrity and attenuating inflammation are critical in protecting intestinal health.

Stimulator of interferon genes (STING) is present in various immune cells and in the enteric nervous system, and its dysregulation affects gastrointestinal motility and is associated with an impaired intestinal barrier (Balasubramaniam *et al.*, 2023). Nuclear factor kappaB (NF-κB) is essential in regulating both the innate and adaptive immune responses by acting as a transcription factor (Yu *et al.*, 2020). NF-κB pathway is linked to numerous illnesses, like cardiovascular disease and cancer, serving as a key pathway in mediating the inflammatory response (Lalle *et al.*, 2021, Cheng *et al.*, 2023). STING activation causes the stimulation of NF-κB pathway, subsequently amplifying the inflammatory reaction (Zhang *et al.*, 2023). Notably, STING/NF-κB pathway is linked to mediate entero virus infection, resulting in a range of intestinal diseases and disrupts intestinal homeostasis (Nigg *et al.*, 2024, Rodwell *et al.*, 2024). It follows that blocking the STING/NF-κB pathway may be beneficial in protecting the integrity of the intestinal barrier.

Over the past few decades, natural products derived from plants have been extensively utilized for treating different

**Corresponding author:* e-mail: qijia265@163.com

illnesses, showing great potential especially in anti-inflammation (Moudgil *et al.*, 2022, Nair *et al.*, 2024). For example, natural products such as quercetin, luteolin and paeoniflorin have been shown to have the ability to reduce inflammation in IBD (Wu *et al.*, 2019, Suga *et al.*, 2021, Hu *et al.*, 2022). Lycorine (LYC) is an isoquinoline alkaloid found in Amaryllidaceae, exhibits diverse biological effects like anti-inflammatory, antiviral, and anti-cancer properties (Xiao *et al.*, 2022, Di Sotto *et al.*, 2023). Liang *et al.* found that LYC could effectively inhibit bleomycin-induced inflammation and alleviate pulmonary fibrosis (Liang *et al.*, 2020). According to a study by Tuo *et al.*, LYC was found to block the phosphoinositol-3-kinase/protein kinase B/NF-κB pathway, which in turn reduced Ang II-induced cardiac dysfunction and effectively alleviated myocardial hypertrophy and fibrosis, as well as cardiac inflammation in mice (Tuo *et al.*, 2024). However, it remains unknown whether LYC improves intestinal barrier integrity and alleviates intestinal inflammation.

As a major part of gram-negative bacterial endotoxin, Lipopolysaccharide (LPS) causes altered permeability of intestinal epithelial cells and triggers IBD and is commonly used to induce intestinal epithelial cell injury models (Stephens *et al.*, 2020, Chen *et al.*, 2023a). Caco-2 cells spontaneously differentiate into intestinal epithelial cells under conventional cell culture conditions, forming a continuous monolayer that is commonly used to mimic the intestinal tract *in vitro* (Lopez-Escalera *et al.*, 2022). Therefore, we constructed a model of LPS-induced Caco-2 cell injury to explore whether LYC alleviates cellular inflammation and intestinal epithelial barrier dysfunction through the STING/NF-κB pathway. This research sought to elucidate the functioning of LYC in reducing intestinal inflammation and to offer valuable insights for the application of LYC and the management of intestinal inflammation.

MATERIALS AND METHODS

Cell culture and treatment

Caco-2 cells (SNL-068) were acquired from Sunncell Biotechnology Co., Ltd.(Wuhan, Hubei, China). Before testing, cells were grown in a mixture of DMEM medium (11965092, Gibco, Grand Island NY, USA), 1% penicillin/streptomycin double antibiotics (15140122, Gibco) and 20% fetal bovine serum (A5670701, Gibco). The interval between fluid changes was 3 days and the passaging ratio was 1:3. The cell culture temperatures were all 37°C, containing 5% CO_2 by volume.

In the LYC cytotoxicity assay, the concentration of LYC (HY-N0288, Med Chem Express, Monmouth Junction, NJ, USA) was 2.5, 5, 10, 20, or 40μM and the treatment time was 24h. In the subsequent Caco-2 cell biological characterization assay cells were exposed to LPS (10μg/mL, HY-D1056, Med Chem Express) for 24 h in the LPS group. Cells in the LPS+LYC group were exposed to LYC for 2h prior to incubation with LPS (10μg/mL) for 24 h.

STING overexpression plasmid (STING) and empty plasmid (Vector) were provided by Sangon Biotech (Shanghai, China). The plasmids mentioned above were introduced into Caco-2 cells using Lipofectamine 3000 (L3000150, Invitrogen, Carlsbad, CA, USA), and the transfection procedure was referred to the instructions. After a 48-hour transfection period, the RNA was isolated with Trizol reagent (R0016, Beyotime, Shanghai, China), while STING level was analyzed to evaluate the transfection efficiency.

Cell Counting Kit-8 (CCK-8) assay

Caco-2 cells were seed into 96-well cell culture plates (1.5×10^4 cells/well). When the cells were completely adhesion, the original medium was discarded and 200μL of medium containing LYC or/and LPS was dispensed into each well, followed by a 24-hour cell culture period. Introduced 20μL of CCK-8 reagent (C0038, Beyotime) into every well. Following a 2-hour incubation at 37°C, the OD_{450} values were determined by using a microplate reader (1410101, Thermo Fisher Scientific, Waltham, MA, USA).

Lactate dehydrogenase (LDH) assay

By utilizing the LDH Cytotoxicity Assay Kit (C0016, Beyotime), the cytotoxicity was detected. Cells were inoculated into 96-well cell culture plates (2.0×10^4 cells/well). Upon reaching 80% confluence, the original medium was discarded and 200μL of a new medium with LYC or/and LPS was introduced. After 24 h of incubation and centrifugation, a mixture was prepared by combining 120μL of supernatant with 60μL of LDH assay working solution, followed by a 30-minute incubation period in darkness. Subsequently, the OD_{490} value was determined to calculate the relative LDH release from the cells.

Flow cytometry

After various treatments, Caco-2 cells were gathered, rinsed twice with PBS and carefully combined with 500 μL of Binding Buffer. Following this, 5μL of Annexin-V-FITC (HY-K1073, Med Chem Express) and 5μL of propidium iodide (ST1569, Beyotime) were introduced and left to incubate for 15 min in a light-free environment. Cell apoptosis was identified through flow cytometry (BD FACS Calibur TM, BD biosciences, San Jose, CA, USA).

TUNEL staining

Caco-2 cells from different treatment groups were exposed to 4% paraformaldehyde (P1110, Solarbio, Beijing, China) for half an hour, followed by the addition of PBS containing 0.3% Triton X-100 (P0096, Beyotime) and left to incubate for 5 min. Following two rinses using PBS, TUNEL assay solution (C1086, Beyotime) was gently added drop wisely to evenly cover the cells and

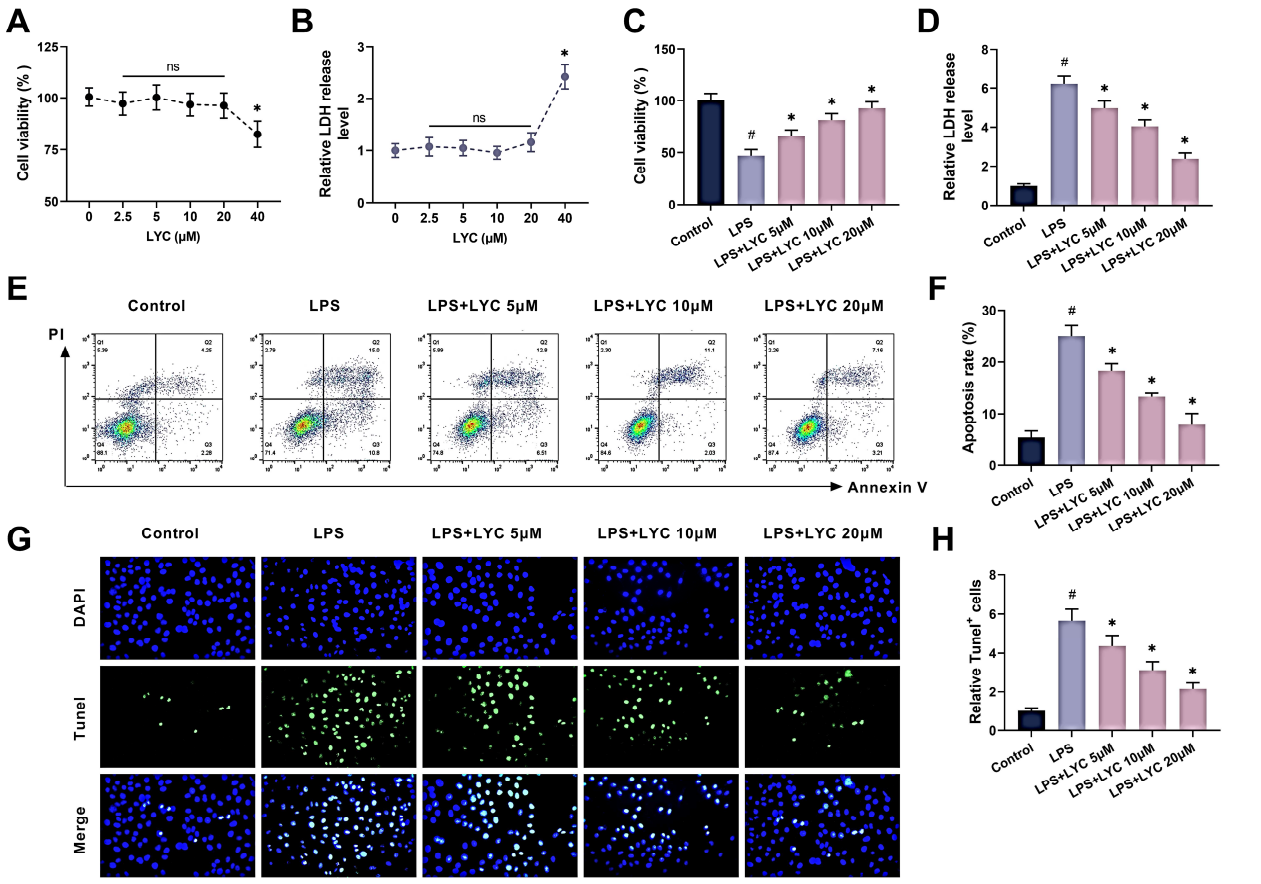

(A) To screen for suitable treatment concentrations, using CCK-8 assay to examine cell viability after 24 h of treatments with different doses of LYC. (B) Cytotoxicity was assessed by LDH assay kit detection of LDH release from Caco-2 cells. (C) CCK-8 assay determined cell viability after LYC or/and LPS treatment. (D) LDH assay kit assessed LDH release from Caco-2 cells following exposure to LYC or/and LPS. (E-F) The apoptosis rate after LYC or/and LPS treatment was assessed by flow cytometry. (G-H) TUNEL staining examined apoptosis after LYC or/and LPS treatment. (#P<0.05 vs Control, *P<0.05 vs LPS)

Fig. 1: LYC attenuates apoptosis in Caco-2 cells induced by LPS

incubated for 1.5 h away from light. Subsequently, added DAPI staining solution (D9542, Sigma-Aldrich, St. Louis, MO, USA) and left to incubate for 10 min without light. After sealing the slides with anti-bursting agent (P0126, Beyotime), inverted fluorescence microscope (DM IL LED, Leica, Heidelberg, Germany) was used to observe and photograph.

ELISA

Utilizing interleukin 1β (IL-1β) (PI303, Beyotime), tumor necrosis factor alpha (TNF-α) (PT516, Beyotime) and interleukin 6 (IL-6) ELISA Kit (PI328, Beyotime) to assess the secretion levels of inflammatory factors in cell supernatants from different groups. The ELISA well plate was filled with the cell culture supernatant and incubated for 2h. After two washes with PBS, added the corresponding antibody and left to incubate for 1h. After that, added HRP-labeled Streptavidin and incubated for 20 min in the darkness, then incubated with TMB solution for 30 min away from light. After adding and thoroughly mixing termination solution, the OD_{450} value was measured and used to calculate the concentration.

Epithelial permeability assay

Well-grown Caco-2 cells were gathered and seed in the chambers of 12-well Transwell plates. The plates were cultured in a incubator for 8 d until the formation of tightly connected monolayers (with medium changes every day), after which the complete medium in the chambers was replaced with medium containing LYC or/and LPS. The resistance values of the cells in each group were determined every 4h using a cell resistivity meter (Millicell ERS-2, Millipore, MA, USA). Three different regions were randomly selected for each measurement and transepithelial electrical resistance (TEER) values were calculated. TEER = (measured resistance data - blank data) × the effective area of Transwell membrane. Caco-2 cells after different treatments were rinsed with PBS twice, the addition of 100μL of FITC-dextran solution (1mg/mL, HY-128868D, Med Chem Express) was followed by an incubation period of 2h at 37°C. The supernatant was obtained after centrifugation, and the intensity of FITC-dextran fluorescence was assessed with a micro plate reader.

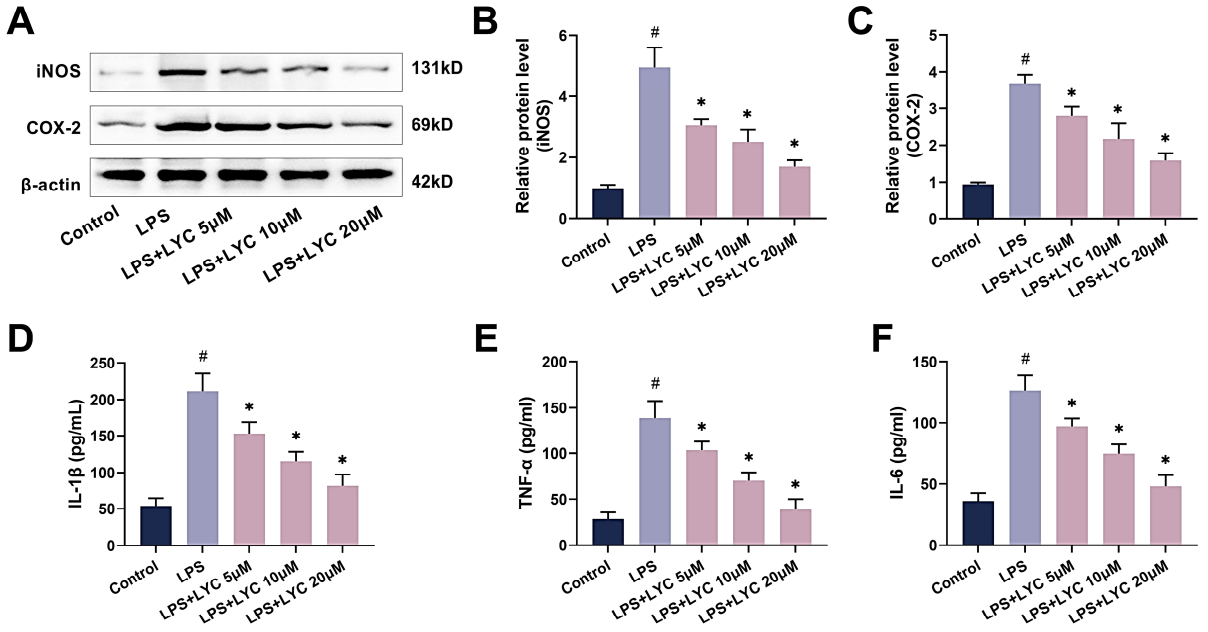

(A-C) Examining iNOS and COX-2 levels in Caco-2 cells via Western blot after different treatments. (D-F) The levels of IL-1β, TNF-α and IL-6 in Caco-2 cells after different treatments were determined by Elisa kit. (#P<0.05 vs Control, *P<0.05 vs LPS)

Fig. 2: LYC attenuates inflammation in Caco-2 cells caused by LPS

Immunofluorescence

Caco-2 cells after different treatments were placed in culture dishes at 2.0×10^4/mL. Once the cells reached a density of 50% to 60%, the culture fluid in the dishes was aspirated, and exposed to 4% paraformaldehyde for 30 min. After exposure to 0.3% Tritonx-100 for 10 min, the cells were enclosed using 5% bovine serum albumin (BSA, ST023, Beyotime) for 40 min. After that, placed at 4ºC for an overnight incubation with zonula occludens-1 (ZO-1) primary antibody (33-9100, 1:300, Invitrogen) or Occludin primary antibody (33-1500, 1:100, Invitrogen). On the following day, after adding FITC-labeled goat anti-rabbit IgG (31460, 1:10000, Invitrogen), the mixture was incubated in darkness for 1 h. Finally, exposed to DAPI solution, kept in darkness for 10 min, and observed by fluorescence microscopy. Fluorescence intensity was obtained after processing the images with Image J software (version 1.54h, Wavne Resband, National Institute of Mental Health, USA).

qRT-PCR

To isolate total RNA, Caco-2 cells were lysed with Trizol reagent. The cDNA was obtained through reverse transcription using AMV reverse transcriptase (2621, TAKARA, Tokyo, Japan). Utilizing the cDNA as a template, the target gene was amplified using TB Green FAST qPCR (CN830S, TAKARA) in a PCR reaction. The relative expression of STING was calculated using $2^{-\Delta\Delta Ct}$ method, with β-actin serving as the internal control.

The following are the primer sequences utilized in this research: STING: F: 5'-GGGAGTGACACACTTGGAT-3'; R: 5'-TCCCAGCACCAGTAAAGCTG-3'. β-actin: F: 5'-TCCTATGGGAGAACGGCAGA-3'; R: 5'-TCCTTT GTCCCCTGAGCTTG-3'.

Western blot

RIPA lysis buffer (P0013B, Beyotime) was utilized for lysing cells or tissues to extract proteins and the BCA kit (P0012, Beyotime) was for assessing protein concentrations. The proteins in the sample underwent electrophoresis on a 12% SDS-PAGE gels (L4509, Sigma-Aldrich), shifted to a PVDF membrane (Invitrogen), followed by blocking with 5% BSA for 2h. After rinsing the membranes, placed at 4ºC for an overnight incubation with inducible nitric oxide synthase (iNOS) primary antibody (PA1-036, 1:1000, Invitrogen), cyclooxygenase-2 (COX-2) primary antibody (35-8200, 1:100, Invitrogen), ZO-1 primary antibody (1:200), Occludin primary antibody (1:1000), Claudin-1 primary antibody (37-4900, 1:100, Invitrogen), p65 primary antibody (51-0500, 1:400, Invitrogen) or p-p65 primary antibody (MA5-15160, 1:1000, Invitrogen).

On the next day, the membranes were cultured with goat anti-rabbit IgG (1:10,000) for 2 h after undergoing three washes. The chemiluminescent agent ECL (34580, Thermo Fisher Scientific) was evenly dispersed on the membrane and observed by a gel imaging system (iBright CL1500, Invitrogen). The grayscale values of each protein band were obtained after processing the images with Image J software, and the relative protein level was quantified by comparison with β-actin (MA1-140, 1:5000, Invitrogen).

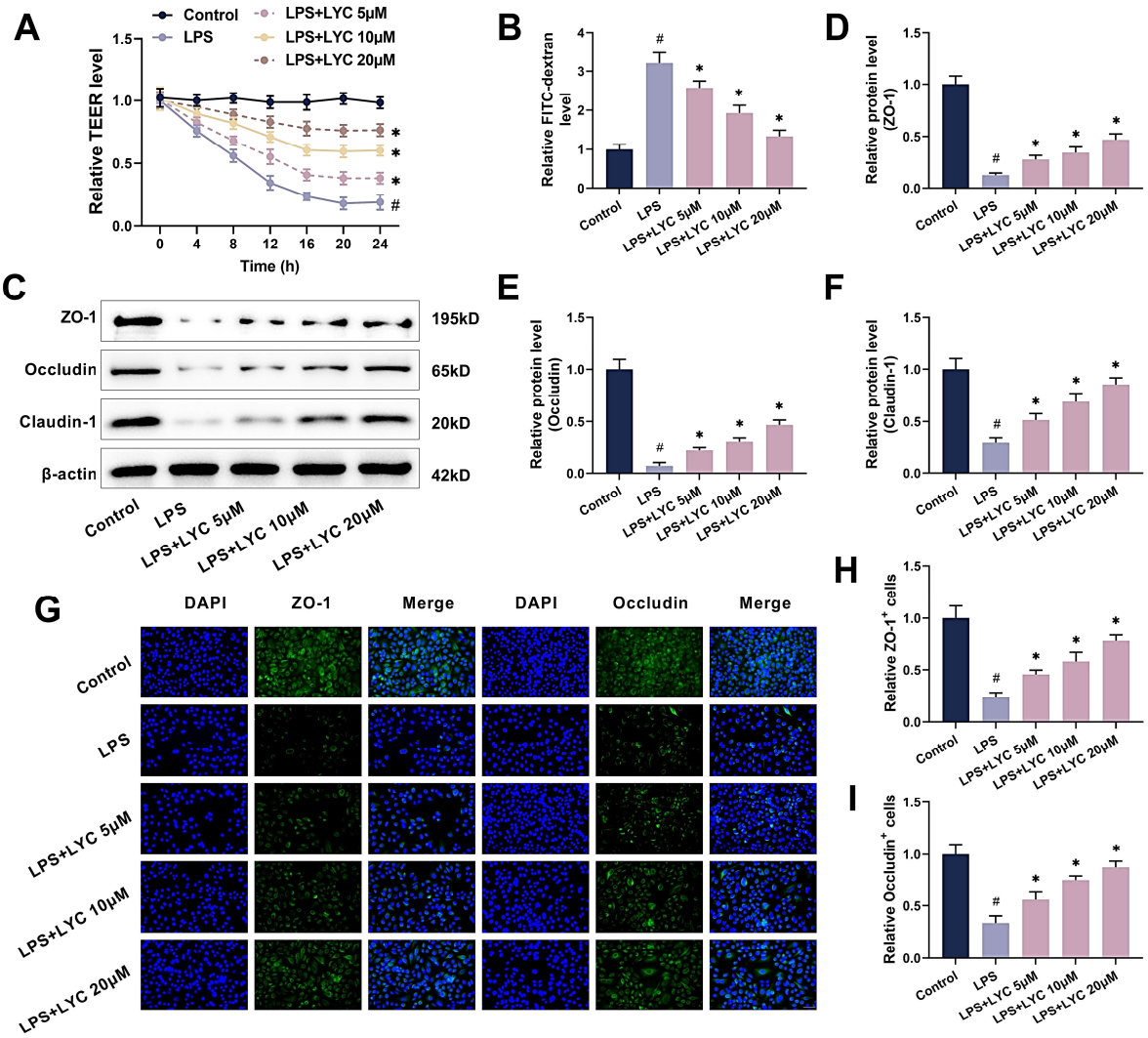

(A) The TEER values were detected by cytoresistance meter following various treatments. (B) Epithelial permeability of Caco-2 cells following various treatments were assessed by FITC-dextran method. (C-F) Examining ZO-1, Occludin and Claudin-1 levels after different treatments through Western blot. (G-I) Immunofluorescence detected the levels of ZO-1 and Occludin. (#P<0.05 vs Control, *P<0.05 vs LPS)

Fig. 3: LYC attenuates epithelial barrier dysfunction in Caco-2 cells induced by LPS

STATISTICAL ANALYSIS

A minimum of 3 repetitions in each experiment, with the result being reported as mean value with the standard deviation. SPSS 26.0 software (IBM SPSS Statistics 26) and Prism software (Graphpad 9.0) for statistical analysis of data and image plotting. The Student's *t*-test was employed to evaluate the contrast between the two groups, while one-way analysis of variance (ANOVA) was utilized to compare multiple groups. P<0.05 denotes significant difference.

RESULTS

LYC reduces the impact of LPS on apoptosis in Caco-2 cells

CCK-8 assay was employed to determine the impacts of varying concentrations of LYC treatment on Caco-2 cell viability for 24h. It was observed that 40μM LYC led to a marked decline in cell viability, indicating that this concentration adversely affected cell growth. However, the cell viability was not notably impacted by LYC as long as the concentration remained below 20μM (fig. 1A). Moreover, at concentrations lower than 20μM, LYC did not show any significant influence on LDH release from Caco-2 cells, whereas 40μM LYC caused a notable elevation in LDH release (fig. 1B). Therefore, in subsequent experiments, we chose 5, 10 and 20μM LYC to treat Caco-2 cells. After being exposed to LPS for 24h, a notable decline in the viability of Caco-2 cells was noted (fig. 1C), and the release of LDH showed a significant rise (fig. 1D). Whereas the addition of LYC weakened the impact of LPS, improved cell viability and reduced LDH release. Flow cytometry findings indicated that LPS treatment caused a notable higher apoptosis rate

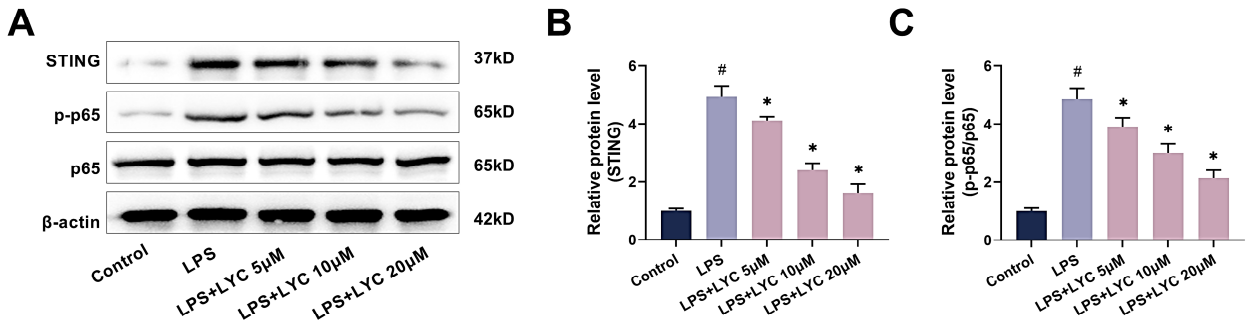

(A) Western blot bands for the pathway proteins STING, p-p65 and p65 in Caco-2 cells. (B-C) The levels of STING, p-p65 and p65 were quantified using Image J software. (#P<0.05 vs Control, *P<0.05 vs LPS)

Fig. 4: LYC hinders the STING/NF-κB pathway in Caco-2 cells

in Caco-2 cells, a effect that was lessened by the addition of LYC (figs. 1E-1F). The number of Tunel-positive Caco-2 cells showed a marked increase upon exposure to LPS, whereas the addition of LYC declined the quantity of Tunel-positive cells and lessened the effect of LPS (figs. 1G-1H). These suggested that LYC was able to attenuate apoptosis in Caco-2 cells with a concentration-dependent effect.

LYC reduces inflammation in Caco-2 cells caused by LPS

The levels of inflammation-related proteins iNOS and COX-2 in Caco-2 cells were detected by Western blot. Following exposure to LPS, there was a notable rise in iNOS and COX-2 levels and LYC (5, 10 and 20μM) suppressed the aberrant expression of inflammation-related proteins (figs. 2A-2C). Following exposure to LPS, Elisa findings indicated a marked rise in the secretion levels of IL-1β, TNF-α and IL-6, which was inhibited by LYC (figs. 2D-2F). These findings demonstrated that LYC significantly suppressed inflammation induced by LPS in Caco-2 cells.

LYC reduces the negative effects of LPS on epithelial barrier in Caco-2 cells

Next, we explored the impact of LYC on epithelial barrier dysfunction caused by LPS. LPS treatment significantly decreased TEER values in Caco-2 cells (fig. 3A) and resulted in increased FITC-dextran levels (fig. 3B), suggesting that LPS negatively affected the function of the epithelial barrier. LYC treatment ameliorated the decline in TEER values and the rise in permeability caused by LPS, demonstrating a protective influence of LYC on the intestinal epithelial barrier. Western blot assay indicated that the levels of ZO-1, Occludin and Claudin-1 were significantly reduced after LPS treatment, while the effect of LPS was weakened by the addition of LYC (figs. 3C-3F). Not only that, by immunofluorescence, after treating Caco-2 cells with LPS, ZO-1 and Occludin levels were markedly declined, which was ameliorated by LYC, in line with the Western blot results (figs. 3G-3I). These findings revealed that treating with LPS caused elevated cell permeability and disruption of the epithelial barrier function and LYC shielded the epithelial barrier against harm caused by LPS.

LYC hinders the STING/NF-κB pathway in Caco-2 cells

To determine the specific mechanisms by which LYC ameliorated inflammation and protected the epithelial barrier, the levels of STING/NF-κB pathway proteins were assessed. After exposure to LPS, the level of STING and the phosphorylation of p65 were notably increased in Caco-2 cells, while LYC dose-dependently decreasing the level of STING and the phosphorylation of p65 (figs. 4A-4C). This demonstrated that LPS triggered the STING/NF-κB pathway, whereas LYC inhibited LPS-induced STING/NF-κB pathway activation.

STING over expression reverses the ameliorative impact of LYC against Caco-2 cell injury caused by LPS

To delve deeper into the influence of the STING/NF-κB pathway in Caco-2 cells, we transfected STING over expression plasmid in Caco-2 cells and assessed the over expression efficiency of STING. The findings indicated that the level of STING was notably elevated in Caco-2 cells after transfection with STING and could be used for subsequent experiments (figs. 5A-5C). LYC (20 μM) inhibited LPS-induced elevated levels of STING as well as phosphorylation of p65, whereas transfection of STING weakened the effect of LYC, suggesting that LYC can effectively inhibit STING/NF-κB pathway activation (figs. 5D-5E). In addition, over expression STING impaired the ameliorative impact of LYC on LPS-induced reduction in Caco-2 cell viability, caused a further reduction in cell viability (fig. 5F), while increased the rate of apoptosis (figs. 5H-5I), promoted the release of LDH (fig. 5G), and elevated the number of Tunel-positive Caco-2 cells (figs. 5J-5K). Altogether, these findings suggested that the STING/NF-κB pathway activation weakened the influence of LYC, demonstrating that LYC could protect Caco-2 cells from damage caused by LPS through blocking the STING/NF-κB pathway.

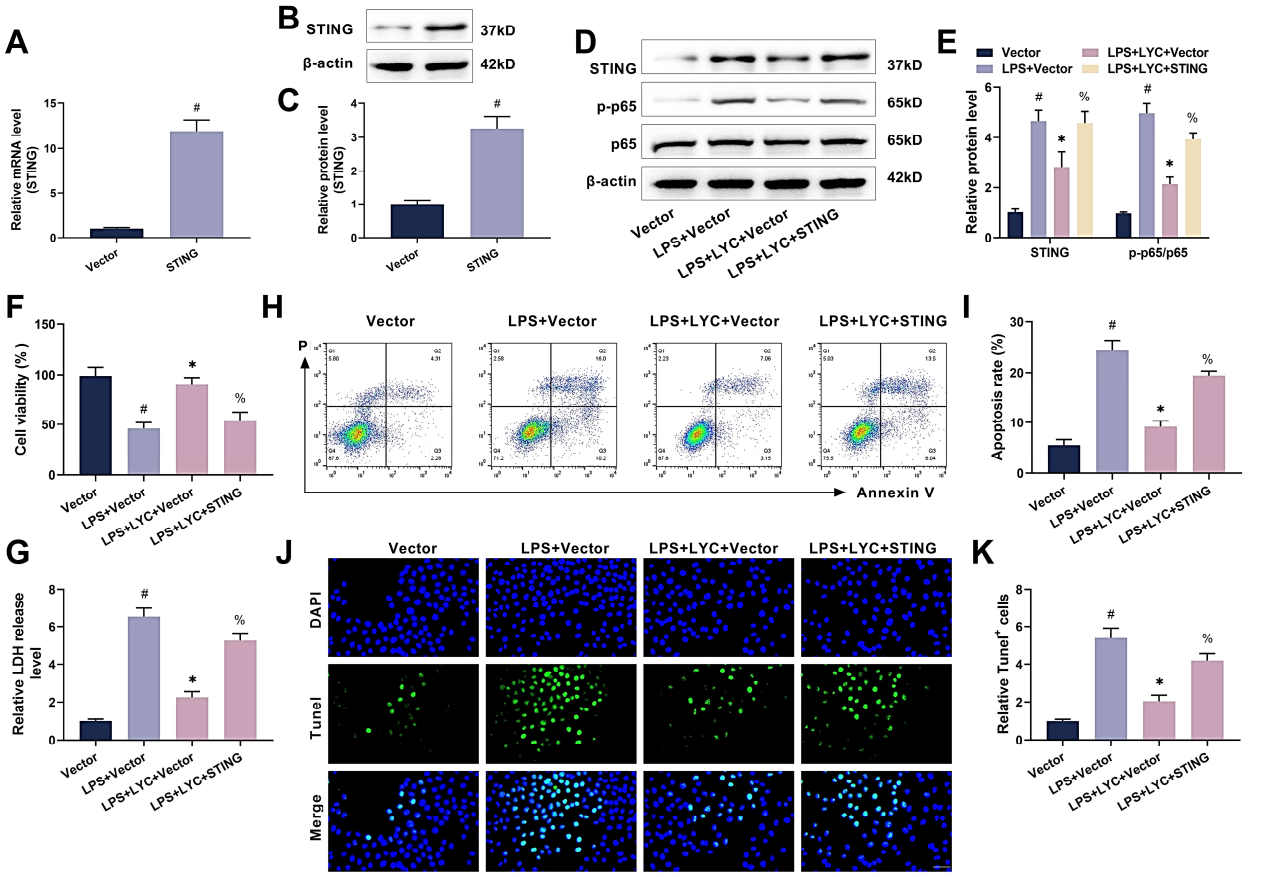

(A) qRT-PCR determined the over expression efficiency of STING after transfection. (B-C) STING expression was assessed through Western blot. (D-E) Examining the levels of pathway proteins STING, p-p65 and p65 in Caco-2 cells after different treatments through Western blot. (F) CCK-8 assay examined the viability of Caco-2 cells following various treatments. (G) LDH assay kit assessed LDH release following various treatments. (H-I) The apoptosis rates were assessed by flow cytometry following various treatments. (J-K) TUNEL staining examined the apoptosis of Caco-2 cells. (#P<0.05 vs Vector, *P<0.05 vs LPS +Vector, %P<0.05 vs LPS +LYC +Vector)

Fig. 5: STING over expression reverses the ameliorative effect of LYC on LPS-induced Caco-2 cell injury

STING over expression reverses the ameliorative effect of LYC on inflammation caused by LPS in Caco-2 cells

Caco-2 cells exhibited a notable rise in iNOS and COX-2 levels after being exposed to LPS treatment, while LYC suppressed the aberrant expression of inflammation-associated proteins and over expression STING caused a further elevation in iNOS and COX-2 levels (figs. 6A-6C). Not only that, LYC suppressed the release of IL-1β, TNF-α, and IL-6 triggered by LPS, whereas over expression STING reversed the influence of LYC (figs. 6D-6F). Above results showed that LYC attenuated inflammation induced by LPS, but over expression STING weakened this effect, suggesting that LYC could ameliorate inflammation through hindering the STING/NF-κB pathway.

STING over expression reverses the ameliorative impact of LYC on epithelial barrier dysfunction

Finally, we explored whether LYC ameliorated epithelial barrier dysfunction through hindering the STING/NF-κB pathway. The findings indicated that LYC treatment suppressed the abnormal reduction of TEER values caused by LPS and decreased FITC-dextran levels in Caco-2 cells, suggesting that LYC could improve LPS-induced epithelial barrier dysfunction (figs. 7A-7B). However, over expression of STING weakened the effect of LYC, decreased TEER values and caused a rise in cell permeability. The levels of ZO-1, Occludin and Claudin-1 were notably declined following LPS treatment, whereas LYC attenuated the effect of LPS, but over expression of STING reversed this phenomenon (figs. 7C-7F). Not only that, the immunofluorescence findings also indicated that over expression STING attenuated the effect of LYC, resulting in a marked reduction of ZO-1 and Occludin levels (figs. 7G-7I). Above findings confirmed that LYC ameliorated epithelial barrier dysfunction through hindering the STING/NF-κB pathway.

DISCUSSION

IBD is a prevalent intestinal disorder affects approximately 1 percent of the world's population,

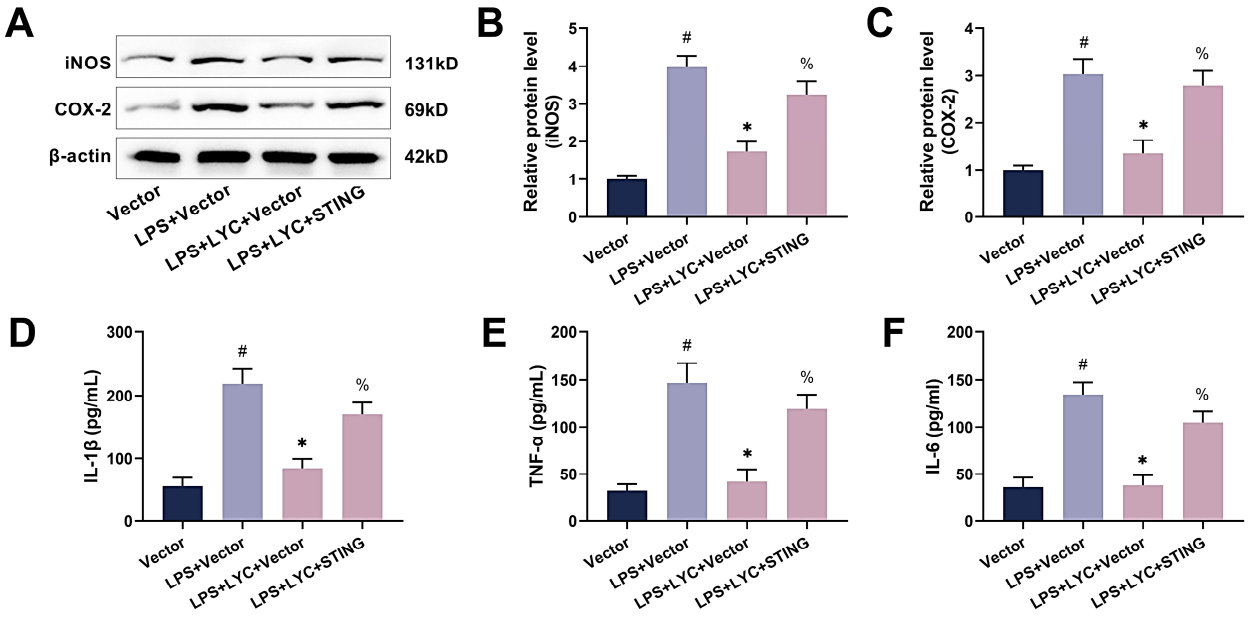

(A-C) Examining the levels of iNOS and COX-2 through Western blot after different treatments. (D-F) The levels of IL-1β, TNF-α and IL-6 in Caco-2 cells were examined using different Elisa kits. (#P<0.05 vs Vector, *P<0.05 vs LPS +Vector, %P<0.05 vs LPS +LYC +Vector)

Fig. 6: STING over expression reverses the ameliorative effect of LYC on inflammation in Caco-2 cells

characterized by abdominal pain, bloody stools, diarrhea, as well as inflammation and ulcers, which can severely affect quality of life(Guan, 2019, Bruner *et al.*, 2023). Inhibition of inflammation is considered an important strategy to slow down the progression of IBD. An investigation indicated that LYC hindered the generation of inflammatory cytokines and inhibited the phosphorylation of NF-κB, suggesting that LYC can help prevent and reduce inflammation-related diseases (Wu *et al.*, 2021). Therefore, in this study, we first screened for suitable LYC treatment concentrations and found that concentrations of LYC below 20 μM did not impact the viability and LDH release of Caco-2 cells. Additionally, LPS treatment reduced the cell viability, resulting in a significant increase in LDH release and apoptosis of Caco-2 cells, whereas LYC attenuated the effect of LPS, suggesting that LYC could protect Caco-2 cell injury induced by LPS.

Nitric oxide (NO) synthesis in the organism is dependent on nitric oxide synthase. Inflammatory cells show a high level of iNOS and activated iNOS produces large amounts of NO, causing tissue damage and disruption of tight junction structures (Kamalian *et al.*, 2020). COX-2, an essential enzyme involved in inflammation, is activated by inflammatory cytokines, further promotes the inflammatory response (Oliveira *et al.*, 2024). TNF-α, a well-known inflammatory factor, is crucial in advancing IBD (Wang *et al.*, 2023a). Not only that, pro-inflammatory factors like IL-6 and IL-1β recruit immune cells to the infection or injury location to promote inflammation, and are important mediators of IBD and tissue injury (Elhag *et al.*, 2022, Chen *et al.*, 2023b). Evidences suggested that LPS promotes the synthesis of inflammatory mediators like iNOS, TNF-α and COX-2 in IBD, leading to immune dysregulation and compromising the intestinal barrier (Candelli *et al.*, 2021, Wang *et al.*, 2022). Ge *et al.* revealed that LYC reduced inflammatory factors in the bronchoalveolar lavage fluid of mice and offered defense against acute lung injury induced by LPS (Ge *et al.*, 2020). In this study, exposure to LPS caused elevated iNOS and COX-2 levels and promoted the production of IL-1β, TNF-α, and IL-6 in Caco-2 cells, aligning with previous study outcomes. LYC treatment reduced the levels of these inflammatory mediators, suggesting that LYC can inhibit LPS-mediated inflammatory responses, suggesting its potential for the treatment of IBD.

In addition to a sustained inflammatory response, intestinal barrier dysfunction is a crucial pathogenesis of IBD(Cheng *et al.*, 2022). The health of the organism relies heavily on the integrity of the intestinal barrier, and TEER serves as a crucial measure of barrier integrity (Schoultz *et al.*, 2020). This study found that LPS treatment decreased TEER values and led to increased intracellular FITC-dextran levels, suggesting that LPS resulted in impaired epithelial barrier and increased cell permeability, while LYC significantly ameliorated LPS-induced epithelial barrier dysfunction. The selective permeability barrier formed by the intestinal monolayer of epithelial cells not only supports nutrient absorption and

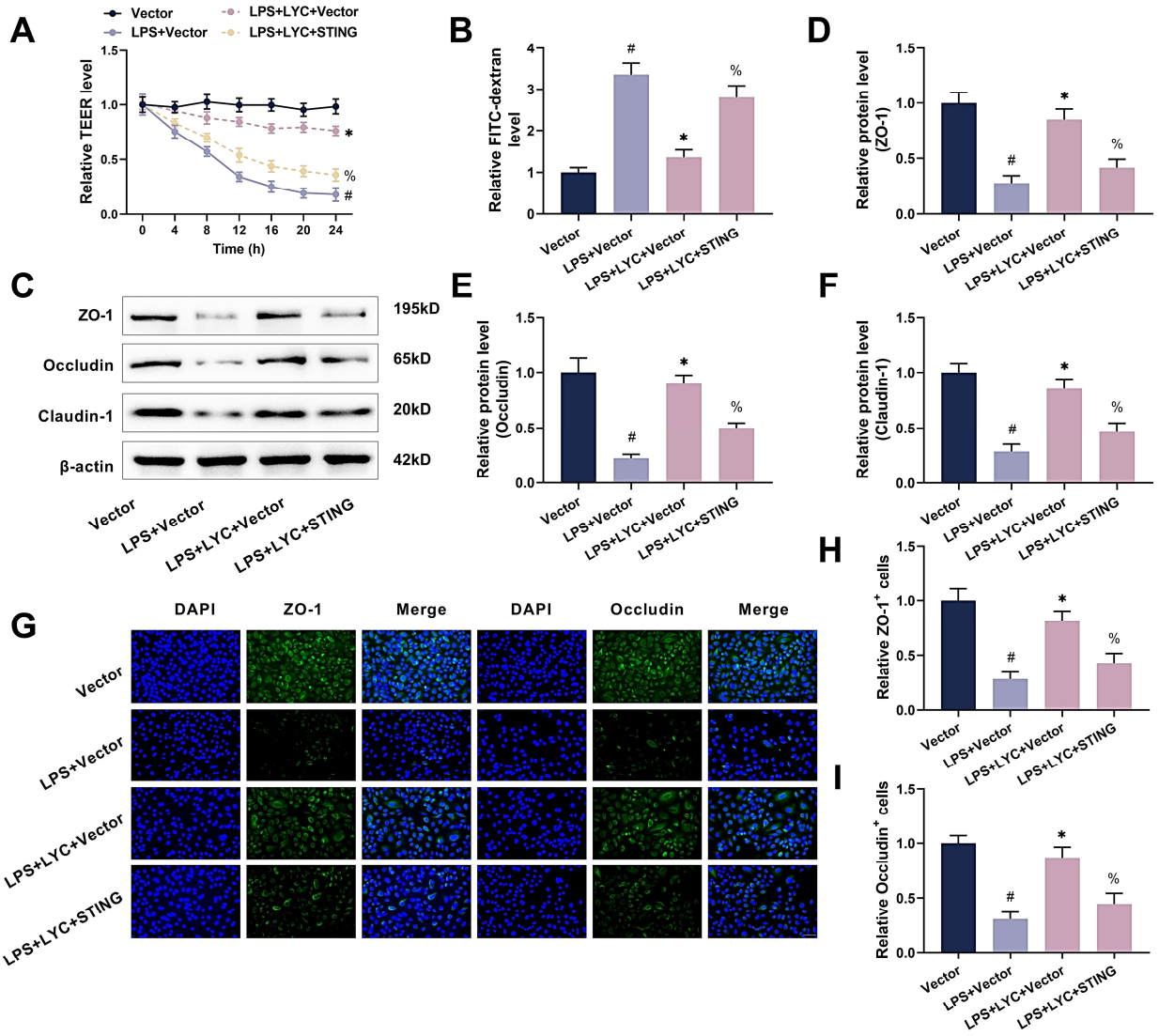

(A) The TEER values were detected by cytoresistance meter following various treatments. (B) After different treatments, the epithelial permeability of Caco-2 cells was assessed by FITC-dextran method. (C-F) Examining ZO-1, Occludin and Claudin-1 levels through Western blot after different treatments. (G-I) Immunofluorescence examined the levels of ZO-1 and Occludin. (#P<0.05 vs Vector, *P<0.05 vs LPS +Vector, %P<0.05 vs LPS +LYC +Vector)

Fig. 7: STING over expression weakens the ameliorative effect of LYC on epithelial barrier dysfunction in Caco-2 cells

waste excretion, but also prevents the entry of harmful substances from the outside world and TJ is essential for the formation of this barrier (Suzuki, 2020, Dunleavy *et al.*, 2023). Among them, ZO-1 interacts with Occludin, Claudin-1, etc. to create strong connections, which collaborate with intracellular signaling proteins to activate relevant pathways to maintain barrier integrity (Chelakkot *et al.*, 2018). The results of this research showed that LPS treatment caused a notable decline in ZO-1, Occludin and Claudin-1 levels, whereas the effect of LPS was weakened by the addition of LYC, which suggests that LYC has a shielding impact on the epithelial barrier against harm caused by LPS.

A growing number of researches highlights the involvement of the STING/NF-κB pathway in the inflammatory processes of different diseases, including cerebral ischemia/reperfusion, cancer and heart failure (Wang *et al.*, 2023b, Yu *et al.*, 2023, Wang *et al.*, 2024). STING/NF-κB signaling activation triggers multiple intestinal diseases including IBD (Nigg *et al.*, 2024, Rodwell and Chtarbanova, 2024). In addition, NF-κB signaling enhances the transcription of different inflammatory cytokines like IL-6, IL-8, and TNF-α. p65 is a key member in NF-κB signaling(Giridharan *et al.*, 2018). This study investigated if LYC shields Caco-2 cells by hindering the STING/NF-κB pathway, given its significance in inflammation. The outcomes of this research showed that LPS exposure caused a rise in STING level and p65 phosphorylation level in Caco-2

cells, indicating that LPS activated the STING/NF-κB pathway. In contrast, LYC attenuated the effect of LPS, suggesting that LYC blocked STING/NF-κB pathway activation. Not only that, we transfected STING over expression plasmid in Caco-2 cells and discovered that over expression STING impaired the ability of LYC to alleviate cellular inflammation and epithelial barrier integrity. This further confirmed that LYC ameliorated LPS-induced inflammation and epithelial barrier dysfunction through suppressing the STING/NF-κB pathway.

CONCLUSION

In summary, LYC attenuated apoptosis and inflammation caused by LPS and protected the epithelial barrier in Caco-2 cells. Notably, the STING/NF-κB pathway activation impaired the protective impact of LYC, confirming that LYC protects Caco-2 cells through hindering the STING/NF-κB pathway. This research provides some theoretical basis for elucidating the mechanism of action of LYC in attenuating intestinal inflammation through the LPS-induced Caco-2 cell model. However, extensive animal researches are required in the future to verify its safety and efficacy *in vivo*.

ACKNOWLEDGMENTS

This study was financially supported by the Tianjin Health and Science and Technology Project (TJWJ2024MS014) and Tianjin Municipal Education Commission Scientific Research Project (Natural Science) (2022KJ185).

REFERENCES

Balasubramaniam A and Srinivasan S (2023). Role of stimulator of interferon genes (STING) in the enteric nervous system in health and disease. *Neurogastroenterol. Motil.,* **35**(7): e14603.

Bruner LP, White AM and Proksell S (2023). Inflammatory Bowel Disease. *Prim. Care.* **50**(3): 411-427.

Candelli M, Franza L, Pignataro G, Ojetti V, Covino M, Piccioni A, Gasbarrini A and Franceschi F (2021). Interaction between Lipopolysaccharide and Gut Microbiota in Inflammatory Bowel Diseases. *Int. J. Mol. Sci.,* **22**(12): 6242.

Chelakkot C, Ghim J and Ryu SH (2018). Mechanisms regulating intestinal barrier integrity and its pathological implications. *Exp. Mol. Med.,* **50**(8): 1-9.

Chen L, Dai M, Zuo W, Dai Y, Yang Q, Yu S, Huang M and Liu H (2023a). NF-κB p65 and SETDB1 expedite lipopolysaccharide-induced intestinal inflammation in mice by inducing IRF7/NLR-dependent macrophage M1 polarization. *Int. Immunopharmacol.,* **115**: 109554.

Chen Y, Cui W, Li X and Yang H (2021). Interaction between commensal bacteria, immune response and the intestinal barrier in inflammatory bowel disease. *Front. Immunol.,* **12**: 761981.

Chen Y, Ye X, Escames G, Lei W, Zhang X, Li M, Jing T, Yao Y, Qiu Z, Wang Z, Acuna-Castroviejo D and Yang, Y (2023b). The NLRP3 inflammasome: contributions to inflammation-related diseases. *Cell. Mol. Biol. Lett.,* **28**(1): 51.

Cheng W, Cui C, Liu G, Ye C, Shao F, Bagchi AK, Mehta JL and Wang X (2023). NF-κB, A Potential Therapeutic Target in Cardiovascular Diseases. *Cardiovasc. Drugs Ther.* **37**(3): 571-584.

Cheng Y, Hall TR, Xu X, Yung I, Souza D, Zheng J, Schiele F, Hoffmann M, Mbow ML, Garnett JP and Li J (2022). Targeting uPA-uPAR interaction to improve intestinal epithelial barrier integrity in inflammatory bowel disease. *EBio Medicine,* **75**: 103758.

D'Aldebert E, Quaranta M, Sébert M, Bonnet D, Kirzin S, Portier G, Duffas JP, Chabot S, Lluel P, Allart S, Ferrand A, Alric L, Racaud-Sultan C, Mas E, Deraison C and Vergnolle N (2020). Characterization of Human Colon Organoids from Inflammatory Bowel Disease Patients. *Front. Cell Dev. Biol.,* **8**: 363.

Di Sotto A, Valipour M, Azari A, Di Giacomo S and Irannejad H (2023). Benzoindolizidine alkaloids tylophorine and lycorine and their analogues with antiviral, anti-inflammatory and anticancer properties: promises and challenges. *Biomedicines,* **11**(10): 2619.

Dunleavy KA, Raffals LE and Camilleri M (2023). Intestinal barrier dysfunction in inflammatory bowel disease: underpinning pathogenesis and therapeutics. *Dig Dis. Sci.,* **68**(12): 4306-4320.

Elhag DA, Kumar M, Saadaoui M, Akobeng AK, Al-Mudahka F, Elawad M and Al Khodor S (2022). Inflammatory bowel disease treatments and predictive biomarkers of therapeutic response. *Int. J. Mol. Sci.,* **23**(13): 6966.

Ge X, Meng X, Fei D, Kang K, Wang Q and Zhao M (2020). Lycorine attenuates lipopolysaccharide-induced acute lung injury through the HMGB1/TLRs/NF-κB pathway. *3 Biotech* **10**(8): 369.

Giridharan S and Srinivasan M (2018). Mechanisms of NF-κB p65 and strategies for therapeutic manipulation. *J. Inflamm. Res.,* **11**: 407-419.

Guan Q (2019). A comprehensive review and update on the pathogenesis of inflammatory bowel disease. *J. Immunol. Res.,* **2019**, 7247238.

Horowitz A, Chanez-Paredes SD, Haest X and Turner JR. (2023). Paracellular permeability and tight junction regulation in gut health and disease. *Nat. Rev. Gastroenterol. Hepatol.,* **20**(7): 417-432.

Hu S, Zhao M, Li W, Wei P, Liu Q, Chen S, Zeng J, Ma X and Tang J (2022). Preclinical evidence for quercetin against inflammatory bowel disease: A meta-analysis and systematic review. *Inflammopharmacology,* **30**(6): 2035-2050.

Kamalian A, Sohrabi Asl M, Dolatshahi M, Afshari K, Shamshiri S, Momeni Roudsari N, Momtaz S, Rahimi R, Abdollahi M and Abdolghaffari AH (2020). Interventions of natural and synthetic agents in inflammatory bowel disease, modulation of nitric oxide pathways. *World J. Gastroenterol.,* **26**(24): 3365-3400.

Lalle G, Twardowski J and Grinberg-Bleyer Y (2021). NF-κB in cancer immunity: Friend or foe? *Cells,* **10**(2): 355.

Liang Q, Cai W, Zhao Y, Xu H, Tang H, Chen D, Qian F and Sun L (2020). Lycorine ameliorates bleomycin-induced pulmonary fibrosis via inhibiting NLRP3 inflammasome activation and pyroptosis. *Pharmacol. Res.,* **158**: 104884.

Lopez-Escalera S and Wellejus A (2022). Evaluation of Caco-2 and human intestinal epithelial cells as *in vitro* models of colonic and small intestinal integrity. *Biochem. Biophys. Rep.,* **31**: 101314.

Mak WY, Zhao M, Ng SC and Burisch J (2020). The epidemiology of inflammatory bowel disease: East meets west. *J. Gastroenterol. Hepatol.,* **35**(3): 380-389.

Moudgil KD and Venkatesha SH (2022). The anti-inflammatory and immunomodulatory activities of natural products to control autoimmune inflammation. *Int. J. Mol. Sci.,* **24**(1): 95.

Nair JJ and Van Staden J (2024). Anti-inflammatory effects of the plant family Amaryllidaceae. *J. Ethnopharmacol.,* **327**: 117943.

Nigg JC, Castello-Sanjuan M, Blanc H, Frangeul L, Mongelli V, Godron X, Bardin AJ and Saleh MC (2024). Viral infection disrupts intestinal homeostasis via Sting-dependent NF-κB signaling in Drosophila. *Curr. Biol.,* **34**(13): 2785-2800.e2787.

Nighot P and Ma T (2021). Endocytosis of Intestinal Tight Junction Proteins: In Time and Space. *Inflamm. Bowel Dis.,* **27**(2): 283-290.

Oliveira A, Rodrigues LC, Soares da Costa D, Fernandes EM, Reis RL, Neves NM, Leao P and Martins A (2024). COX-2 inhibitor delivery system aiming intestinal inflammatory disorders. *Biomater Adv,* **156**: 213712.

Rodwell M and Chtarbanova S (2024). STING-NF-κB signaling: Viral infection drives gut aging effects. *Curr. Biol.,* **34**(13): R618-r620.

Rohr MW, Narasimhulu CA, Rudeski-Rohr TA and Parthasarathy S (2020). Negative effects of a high-fat diet on intestinal permeability: A review. *Adv. Nutr.* **11**(1): 77-91.

Saez A, Gomez-Bris R, Herrero-Fernandez B, Mingorance C, Rius C and Gonzalez-Granado JM (2021). Innate lymphoid cells in intestinal homeostasis and inflammatory bowel disease. *Int. J. Mol. Sci.,* **22**(14): 7618.

Schoultz I and Keita AV (2020). The intestinal barrier and current techniques for the assessment of gut permeability. *Cells,* **9**(8): 1909.

Shen Q, Huang Z, Yao J and Jin Y (2022). Extracellular vesicles-mediated interaction within intestinal microenvironment in inflammatory bowel disease. *J. Adv. Res.,* **37**: 221-233.

Stephens M and Von der Weid PY (2020). Lipopolysaccharides modulate intestinal epithelial permeability and inflammation in a species-specific manner. *Gut microbes,* **11**(3): 421-432.

Suga N, Murakami A, Arimitsu H, Nakamura T, Nakamura Y and Kato Y (2021). Luteolin suppresses 5-hydroxytryptamine elevation in stimulated RBL-2H3 cells and experimental colitis mice. *J. Clin. Biochem. Nutr.* **69**(1): 20-27.

Suzuki T (2020). Regulation of the intestinal barrier by nutrients: The role of tight junctions. *Anim. Sci. J.,* **91**(1): e13357.

Tuo P, Zhao R, Li N, Yan S, Yang G, Wang C, Sun J, Sun H and Wang M (2024). Lycorine inhibits Ang II-induced heart remodeling and inflammation by suppressing the PI3K-AKT/NF-κB pathway. *Phytomedicine,* **128**: 155464.

Wang J, Macoritto M, Guay H, Davis JW, Levesque MC and Cao X (2023a). The clinical response of upadacitinib and risankizumab is associated with reduced inflammatory bowel disease anti-tnf-α inadequate response mechanisms. *Inflamm. Bowel Dis.,* **29**(5): 771-782.

Wang L, Zhang S, Liu H, Gao L, He L, Chen Y, Zhang J, Yang M and He C (2024). STING activation in cardiomyocytes drives hypertrophy-associated heart failure via NF-κB-mediated inflammatory response. *Biochimica et biophysica acta. Biochim. Biophys. Acta Mol. Basis. Dis.,* **1870**(3): 166997.

Wang X, Chen S, Xiang H, Wang X, Xiao J, Zhao S, Shu Z, Ouyang J, Liang Z, Deng M, Chen X, Zhang J, Liu H, Quan Q, Gao P, Fan J, Chen AF and Lu H (2022). S1PR2/RhoA/ROCK1 pathway promotes inflammatory bowel disease by inducing intestinal vascular endothelial barrier damage and M1 macrophage polarization. *Biochem. Pharmacol.,* **201**: 115077.

Wang X, Huang J, Liu F, Yu Q, Wang R, Wang J, Zhu Z, Yu J, Hou J, Shim JS, Jiang W, Li Z, Zhang Y and Dang Y (2023b). Aurora A kinase inhibition compromises its antitumor efficacy by elevating PD-L1 expression. *J. Clin. Invest.,* **133**(9): e161929.

Wu J, Fu Y, Wu YX, Wu ZX, Wang ZH and Li P (2021). Lycorine ameliorates isoproterenol-induced cardiac dysfunction mainly via inhibiting inflammation, fibrosis, oxidative stress and apoptosis. *Bioengineered,* **12**(1): 5583-5594.

Wu XX, Huang XL, Chen RR, Li T, Ye HJ, Xie W, Huang ZM and Cao GZ (2019). Paeoniflorin prevents intestinal barrier disruption and inhibits lipopolysaccharide (LPS)-induced inflammation in Caco-2 cell monolayers. *Inflammation,* **42**(6): 2215-2225.

Xiao H, Xu X, Du L, Li X, Zhao H, Wang Z, Zhao L, Yang Z, Zhang S, Yang Y and Wang C (2022). Lycorine and organ protection: Review of its potential

effects and molecular mechanisms. *Phytomedicine,* **104**: 154266.

Yu H, Lin L, Zhang Z, Zhang H and Hu H (2020). Targeting NF-κB pathway for the therapy of diseases: mechanism and clinical study. *Signal Transduct. Target Ther.,* **5**(1): 209.

Yu Z, Zheng L, Geng Y, Zhang Y, Wang Y, You G, Cai M, Li M, Cheng X and Zan J (2023). FTO alleviates cerebral ischemia/reperfusion-induced neuro-inflammation by decreasing cGAS mRNA stability in an m6A-dependent manner. *Cell Signal,* **109**: 110751.

Zhang L, Wei X, Wang Z, Liu P, Hou Y, Xu Y, Su H, Koci MD, Yin H and Zhang C (2023). NF-κB activation enhances STING signaling by altering microtubule-mediated STING trafficking. *Cell Rep.,* **42**(3): 112185.

Zhou B, Yuan Y, Zhang S, Guo C, Li X, Li G, Xiong W and Zeng Z (2020). Intestinal flora and disease mutually shape the regional immune system in the intestinal tract. *Front. Immunol.,* **11**: 575.